

UCLA

UCLA Previously Published Works

Title

Proteomic signature of HIV-associated subclinical left atrial remodeling and incident heart failure

Permalink

<https://escholarship.org/uc/item/98f5r3hr>

Journal

Nature Communications, 16(1)

ISSN

2041-1723

Authors

Peterson, Tess E

Hahn, Virginia S

Moaddel, Ruin

et al.

Publication Date

2025

DOI

10.1038/s41467-025-55911-0

Peer reviewed

Proteomic signature of HIV-associated subclinical left atrial remodeling and incident heart failure

Received: 24 April 2024

Accepted: 2 January 2025

Published online: 12 January 2025

 Check for updates

Tess E. Peterson^{1,2,15} ✉, Virginia S. Hahn^{1,15}, Ruin Moaddel³, Min Zhu³, Sabina A. Haberen⁴, Frank J. Palella⁵, Michael Plankey⁶, Joel S. Bader⁷, Joao A. C. Lima¹, Robert E. Gerszten⁸, Jerome I. Rotter⁹, Stephen S. Rich¹⁰, Susan R. Heckbert¹¹, Gregory D. Kirk⁴, Damani A. Piggott^{4,12}, Luigi Ferrucci³, Joseph B. Margolick^{4,13}, Todd T. Brown^{4,14}, Katherine C. Wu^{1,16} & Wendy S. Post^{1,4,16}

People living with HIV are at higher risk of heart failure and associated left atrial remodeling compared to people without HIV. Mechanisms are unclear but have been linked to inflammation and premature aging. Here we obtain plasma proteomics concurrently with cardiac magnetic resonance imaging in two independent study populations to identify parallels between HIV-related and aging-related immune dysfunction that could contribute to atrial remodeling and clinical heart failure. We discover a plasma proteomic signature that may in part reflect or contribute to HIV-associated atrial remodeling, many features of which are associated with older age and time to incident heart failure among an independent community-based cohort without HIV. This proteomic profile was statistically enriched for immune checkpoint proteins, tumor necrosis factor signaling, ephrin signaling, and extracellular matrix organization, identifying possible shared pathways in HIV and aging that may contribute to risk of heart failure.

With improved access to early and effective antiretroviral therapy (ART), HIV has become a chronic condition marked by higher risk and earlier onset of aging-related diseases, including cardiovascular disease (CVD)¹. People living with HIV (PLWH), even those with viral

suppression consequent to ART use, are at higher risk of myocardial diseases², such as incident heart failure (HF)^{3–5} and atrial fibrillation (AF)⁶. Advanced HIV disease has been classically associated with left ventricular (LV) systolic dysfunction and dilated cardiomyopathy, but

¹Division of Cardiology, Department of Medicine, Johns Hopkins University, Baltimore, MD, USA. ²Division of Epidemiology & Community Health, School of Public Health, University of Minnesota, Minneapolis, MN, USA. ³Biomedical Research Centre, National Institute on Aging, NIH, Baltimore, MD, USA.

⁴Department of Epidemiology, Johns Hopkins Bloomberg School of Public Health, Baltimore, MD, USA. ⁵Department of Medicine, Northwestern University Feinberg School of Medicine, Chicago, IL, USA. ⁶Division of General Internal Medicine, Department of Medicine, Georgetown University, Washington, DC, USA. ⁷Department of Biomedical Engineering, Whiting School of Engineering, Johns Hopkins University, Baltimore, MD, USA. ⁸Division of Cardiovascular Medicine, Beth Israel Deaconess Medical Center, Boston, MA, USA. ⁹The Institute for Translational Genomics and Population Sciences, Department of Pediatrics, The Lundquist Institute for Biomedical Innovation at Harbor-UCLA Medical Center, Torrance, CA, USA. ¹⁰Department of Genome Sciences, University of Virginia, Charlottesville, VA, USA. ¹¹Department of Epidemiology, University of Washington School of Public Health, Seattle, WA, USA. ¹²Division of Infectious Diseases, Department of Medicine, Johns Hopkins University, Baltimore, MD, USA. ¹³Division of Molecular Microbiology and Immunology, Department of Medicine, Johns Hopkins University, Baltimore, MD, USA. ¹⁴Division of Endocrinology, Diabetes, and Metabolism, Department of Medicine, Johns Hopkins University, Baltimore, MD, USA. ¹⁵These authors contributed equally: Tess E. Peterson, Virginia S. Hahn. ¹⁶These authors jointly supervised this work: Katherine C Wu, Wendy S Post. ✉e-mail: tpeter@umn.edu

with effective ART, this phenotype has transitioned to one characterized by subclinical abnormalities in cardiac structure and function that may presage clinical HF, particularly HF with preserved ejection fraction (EF)⁷. We previously demonstrated PLWH have a higher risk of diastolic dysfunction and related structural abnormalities compared to people without HIV (PWOH), including subclinical left atrial (LA) enlargement^{8,9}, findings supported by other data across world regions^{10–13}. Indexed left atrial volume (LAVi) reflects the cumulative effect of chronically elevated LV filling pressure and is an independent predictor of diastolic dysfunction and clinical HF¹⁴.

Mechanisms contributing to HIV-associated myocardial disease are hypothesized to be multifactorial, mediated by chronic immune activation and dysfunction that persists despite ART-induced viral suppression. Hypothesized contributors include direct immune activation and exhaustion due to HIV viral persistence and co-pathogens, metabolic dysfunction due to HIV and use of certain antiretrovirals, higher mucosal permeability and microbial translocation, and higher prevalence of risk factors with known pro-inflammatory effects, including substance use⁷. However, it remains unclear to what degree mechanisms underlying this risk differ among PLWH compared to PWOH, among whom aging-related immunosenescence and inflammaging may similarly contribute to clinical HF risk. Moreover, therapeutic and preventive strategies among PLWH, particularly for HF, are largely guided by data from clinical trials conducted among PWOH, so

evaluating this knowledge gap may have important clinical implications.

Proteomics provides a high-throughput discovery approach to generate mechanistic hypotheses that could lead to improved risk prediction, disease characterization, and targeted pharmacologic therapies. We performed proteomic analyses using the Olink Explore 3072 platform on stored plasma obtained concurrently with cardiovascular magnetic resonance (CMR) among largely ART-treated and virally suppressed PLWH and sociodemographically similar PWOH enrolled in the Subclinical Myocardial Abnormalities in HIV (SMASH) study⁹, the discovery cohort. Our objective was to identify plasma proteomic signatures that may represent markers of HIV-associated atrial remodeling, defined as features associated with both positive HIV serostatus and higher LAVi. We then sought to evaluate whether identified proteomic signatures were associated with LAVi, incident AF, and incident adjudicated HF among a large external cohort of older PWOH in the Multi-Ethnic Study of Atherosclerosis (MESA). Here, we discover such a proteomic signature that may in part reflect or contribute to HIV-associated atrial remodeling, many features of which are associated with older age and time to incident heart failure in the MESA. This signature is enriched in immune checkpoint proteins, tumor necrosis factor signaling, ephrin signaling, and extracellular matrix organization, which may help identify shared mechanistic pathways in HIV and aging that contribute to a higher risk of clinical HF.

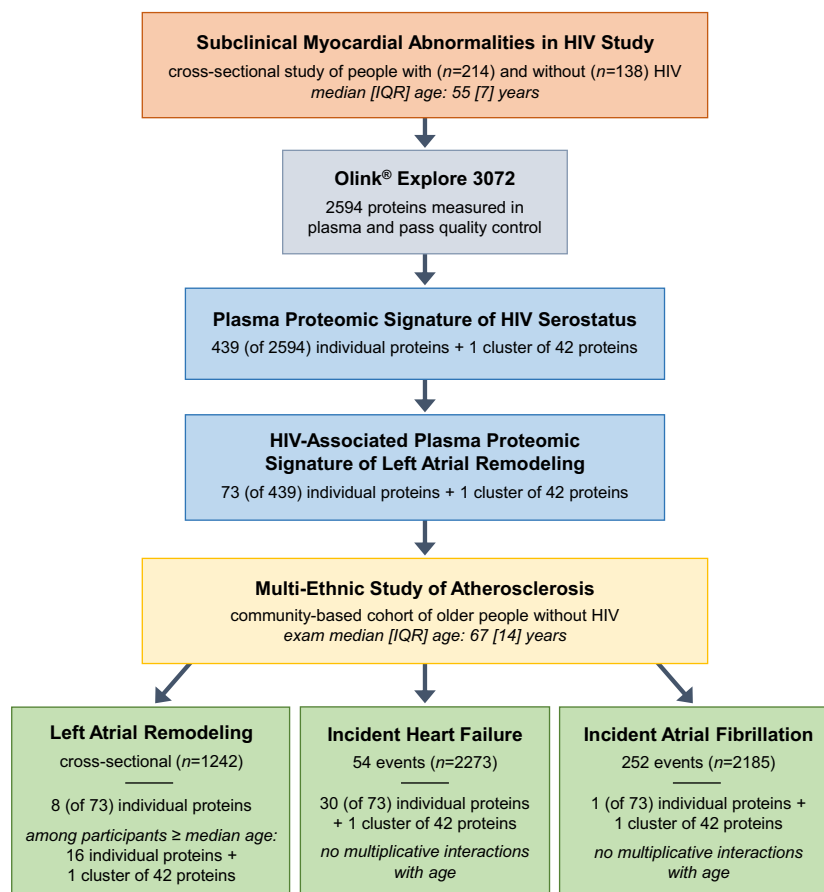


Fig. 1 | Graphical representation of the study design and analytic flow. Cross-sectional discovery analyses were performed in the Subclinical Myocardial Abnormalities in HIV Study (SMASH) using linear regression with robust variance. Analyses of HIV serostatus adjusted for sociodemographics, substance use, hepatitis C virus infection, and renal function. Analyses of left atrial size further adjusted for HIV serostatus, body mass index, systolic blood pressure, hypertension medication use, dyslipidemia, and diabetes. Both cross-sectional and longitudinal time-to-incident event analyses were performed among an external population of older

people without HIV in the Multi-Ethnic Study of Atherosclerosis (MESA). Cross-sectional analyses of left atrial size were performed using linear regression with robust variance, adjusting for field center, sociodemographics, smoking, body mass index, systolic blood pressure, hypertension medication use, dyslipidemia, diabetes, and renal function. Time-to-event analyses of atrial fibrillation and heart failure were performed using Cox proportional hazards regression, adjusting for the same covariates. Proteome feature counts listed are those associated with indicated outcomes at a false discovery rate < 0.05.

Table 1 | SMASH participant characteristics by HIV serostatus (n = 352)

CHARACTERISTIC	Median [IQR] or % (n)		p-value
	PLWH (n = 214)	PWOH (n = 138)	
Study site	–	–	–
MACS Baltimore	75 (35%)	46 (33%)	0.75
MACS Chicago	28 (13%)	17 (12%)	
WIHS	39 (18%)	21 (15%)	
ALIVE	72 (34%)	54 (39%)	
Demographics			
Age, years	55 [51,58]	55 [52,58]	0.34
Female sex at birth	55 (26%)	34 (25%)	0.90
Race and ethnicity			
Black, non-Hispanic	151 (71%)	94 (68%)	0.79
White, non-Hispanic	52 (24%)	34 (25%)	
Hispanic	11 (5%)	10 (7%)	
Education level ≥ high school	156 (73%)	108 (78%)	0.30
Substance Use			
Smoking status			
Current	114 (53%)	57 (41%)	0.14
Former	56 (26%)	57 (41%)	
Never	44 (21%)	24 (17%)	
Pack-years of smoking ^a	0.99 [0.00, 2.82]	0.21 [0.00, 2.16]	0.06
Hazardous alcohol use (AUDIT score >8)	23 (11%)	20 (14%)	0.39
Opioid use ^a	61 (29%)	47 (34%)	0.34
Stimulant use ^a	87 (41%)	50 (36%)	0.45
Clinical Factors			
History of cardiovascular disease	14 (7%)	8 (6%)	0.99
Body mass index, kg/m ²	25.7 [23.0, 29.3]	26.9 [24.1, 31.0]	0.04
Hypertension ^b	108 (51%)	74 (54%)	0.61
Systolic blood pressure, mmHg	124 [118, 134]	128 [121, 135]	0.02
Blood pressure-lowering medication use	74 (35%)	49 (36%)	0.70
Dyslipidemia ^c	130 (61%)	77 (56%)	0.44
Total cholesterol, mg/dL	172 [149, 195]	177 [151, 208]	0.04
High density lipoprotein cholesterol, mg/dL	51 [41,63]	58 [46,69]	0.02
Lipid-lowering medication use	54 (25%)	31 (23%)	0.70
Diabetes ^d	27 (13%)	16 (12%)	0.87
Diabetes medication use	20 (9%)	12 (9%)	0.99
eGFR, CKD-EPI, mL/min/1.73 m ²	89 [74, 103]	93 [78, 106]	0.12
Hepatitis C diagnosis	50 (23%)	28 (20%)	0.51
Cardiovascular Magnetic Resonance			
LV ejection fraction, %	72 [67,76]	72 [68,76]	0.19
LV ejection fraction < 50%	4 (2%)	0 (0%)	–
LV mass indexed by BSA, mg/m ²	61.8 [56.8, 68.6]	61.7 [55.8, 67.0]	0.28
LV end-diastolic volume indexed by BSA, mL/m ²	67.6 [58.0, 77.0]	64.4 [54.3, 76.2]	0.11
LA volume indexed by BSA, mL/m ²	28.1 [22.1, 35.8]	26.7 [22.6, 32.9]	0.06
LA volume indexed by BSA ≥ 40 mL/m ²	32 (15%)	8 (6%)	0.02

Table 1 (continued) | SMASH participant characteristics by HIV serostatus (n = 352)

CHARACTERISTIC	Median [IQR] or % (n)		p-value
	PLWH (n = 214)	PWOH (n = 138)	
LA volume indexed by BSA ≥ 53 mL/m ²	6 (3%)	2 (1%)	–
Late gadolinium enhancement	81 (38%)	46 (33%)	0.44
Extracellular volume fraction, %	28.9 [26.5, 31.2]	28.2 [26.1, 29.9]	0.04
HIV-Related Factors			
HIV viral load detectable (> 50 RNA copies/mL)	55 (26%)	–	–
CD4 + T cell count, cells/μL	605 [400, 815]	–	–
CD4+ nadir T cell count, cells/μL	271 [149, 386]	–	–
History of AIDS diagnosis	29 (20%)	–	–
ART use			
Duration of ART, years	12.8 [5.4, 16.0]	–	–
Protease inhibitor base	75 (35%)	–	–
Non-nucleoside reverse transcriptase inhibitor base	57 (27%)	–	–
Integrase strand inhibitor base	53 (25%)	–	–
Other ART base	3 (1%)	–	–

p-values computed for two-sided differences in distribution by HIV serostatus using the Wilcoxon rank-sum or t test and Pearson's or Fisher's χ^2 test for continuous and categorical variables, respectively.

^a Reported in the five years preceding cardiovascular magnetic resonance imaging (CMR).

^b Hypertension is defined as the use of antihypertensive medication or systolic blood pressure ≥ 140 mmHg or diastolic blood pressure ≥ 90 mmHg averaged over the preceding 5 years when available or at the time of CMR study visit.

^c Dyslipidemia is defined as the use of lipid-lowering medication or fasting total cholesterol level ≥ 200 mg/dL or low-density lipoprotein cholesterol level ≥ 130 mg/dL or high-density lipoprotein cholesterol level < 40 mg/dL or serum triglyceride level ≥ 150 mg/dL closest to the time of CMR study visit.

^d Diabetes is defined as the use of hypoglycemic medication or fasting serum glucose levels ≥ 126 mg/dL closest to the time of the CMR study visit. Hemoglobin A1C level < 6.5% was used to exclude diabetes if fasting glucose levels were not available.

PLWH = people living with HIV; PWOH = people without HIV; IQR = interquartile range, reported as [25th, 75th] percentiles; AUDIT = Alcohol Use Disorders Identification Test; eGFR = estimated glomerular filtration rate; LV = left ventricular; LA = left atrial; BSA = body surface area; ART = antiretroviral therapy.

Results

A graphical representation of the study design and analytic flow is depicted in Fig. 1.

SMASH Participant characteristics

Of 468 persons initially enrolled in SMASH, 352 were selected for plasma proteomics based on the availability of complete CMR data, including gadolinium enhancement, and adequate stored plasma volume (Supplementary Fig. S1). Selected participants had a lower representation of females and a lower prevalence of hypertension and hepatitis C virus infection (HCV) compared to unselected participants (Supplementary Table S1). Demographic, clinical, and CMR characteristics of selected participants are summarized in Table 1 by HIV serostatus and by cohort in Supplementary Table S2. Participants were mean (standard deviation, SD) age 55 (6) years old, 25% female, 61% PLWH, and had predominantly normal LVEF. LAVi was higher among PLWH compared to PWOH—29.7 (11.3) and 27.7 (8.3) mL/m², respectively ($p = 0.02$ for difference, adjusting for demographics, substance use, and traditional CVD risk factors).

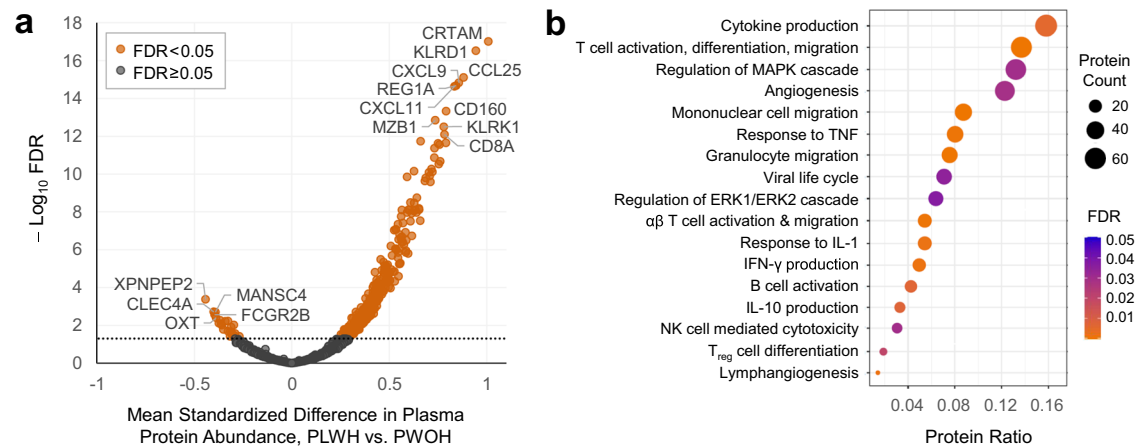


Fig. 2 | Proteomic signature of HIV seropositivity among people living with and without HIV in the United States ($n = 352$). **a** Volcano plot of mean differences in standardized plasma protein abundance comparing PLWH to PWOH vs. $-\log_{10}$ false discovery rate (FDR; Benjamini-Hochberg) estimated using linear regression with robust variance, adjusting for sociodemographics, substance use, hepatitis C virus infection, and renal function. The threshold for significance is indicated by a gray dotted line, $FDR < 0.05$; 415 of 2596 proteins were positively associated with positive HIV serostatus and 24 proteins were inversely associated; comparing suppressed PLWH vs. PWOH, 414 of these 439 total proteins were associated with

suppressed positive HIV serostatus (not depicted). Complete modeling results can be found in Supplementary Data 1. **b** Enriched biological processes among proteins associated with HIV serostatus, estimated using a two-sided Fisher's exact test, Gene Ontology: Biological Processes annotations, and a threshold for significance of $FDR < 0.05$. Protein ratio = proportion of proteins significantly associated with HIV serostatus ($n = 439$) that map to the given annotation. Proteins mapping to each annotation can be found in Supplementary Table S3. PLWH = persons living with HIV; PWOH = persons without HIV; suppressed HIV viral load = HIV RNA < 50 copies/ μ L.

Proteomic signature of HIV serostatus

Of 2596 proteins analyzed, plasma abundances of 439 proteins were significantly associated with positive HIV serostatus following multivariable adjustment (415 positively associated and 24 inversely associated with a false discovery rate, $FDR < 0.05$) (Fig. 2). These proteins were statistically enriched for many biological processes, including T cell activation, differentiation, and migration; B cell activation; natural killer (NK) cell-mediated cytotoxicity; regulation of mitogen-activated protein kinase (MAPK) and extracellular signal-regulated kinase 1/2 (ERK1/ERK2) cascades; tumor necrosis factor (TNF) signaling; response to interleukin (IL)-1; IL-10 production; and interferon- γ (IFN- γ) production. The strongest association with HIV was that of cytotoxic and regulatory T cell molecule (CRTAM); on average, its adjusted plasma abundance was 1.01 SD higher among PLWH compared to PWOH (95% confidence interval [CI]: 0.84–1.17; $FDR = 1.70 \times 10^{-29}$). Upon exclusion of viremic PLWH, 414 of these 439 proteins remained significantly associated with positive HIV serostatus (390 positively, 24 inversely), among the strongest of which was CRTAM ($FDR = 1.51 \times 10^{-20}$). See Supplementary Data 1 for complete results of protein associations with HIV serostatus and Supplementary Table S3 for enrichment details.

Many classical markers reflecting chronic immune activation and systemic inflammation among PLWH were significantly elevated among PLWH compared to PWOH, including the monocyte activation markers soluble CD14 ($FDR = 2.60 \times 10^{-10}$) and CD163 ($FDR = 0.009$), as well as CXCL10 ($FDR = 1.73 \times 10^{-8}$) and TNFR1 ($FDR = 0.014$). Notably, IL-6 levels did not differ by HIV serostatus ($p = 0.19$, $FDR = 0.42$), consistent with previously reported immunoassay results among this study population¹⁵. These inferences were unchanged following the exclusion of viremic PLWH.

Of six protein clusters agnostically identified using weighted gene co-expression network analysis (WGCNA) (details in Supplementary Data 2, Supplementary Table S4 and Supplementary Fig. S2), higher plasma abundance of one cluster (Brown) was independently associated with positive HIV serostatus ($p = 3.99 \times 10^{-6}$), and this association remained following exclusion of viremic PLWH ($p = 1.02 \times 10^{-4}$) (Supplementary Table S5). This cluster comprised 42 proteins

enriched for regulation of T cell proliferation, TNF signaling, ephrin signaling, cell-cell adhesion, and extracellular matrix (ECM) organization (Supplementary Table S6).

HIV-Associated proteomic signature of left atrial remodeling

Next, we identified proteome features significantly associated with both HIV serostatus and LAVi that may reflect potential contributors to or biomarkers of HIV-associated LA remodeling. Of 439 proteins associated with HIV serostatus, 78 were also associated with LAVi (74 positively, 4 inversely), adjusting for demographics, substance use, HIV, HCV, and estimated glomerular filtration rate (eGFR). Upon further adjustment for traditional CVD risk factors, 73 remained associated (69 positively, 4 inversely) (Fig. 3a and Supplementary Data 3), all of which were associated with concordant directionality compared to positive HIV serostatus (Fig. 3b). In subgroup analyses, 72 (99%) of these proteins differed in mean plasma level between virally suppressed PLWH and PWOH. These proteins were statistically enriched for involvement in T cell activation, differentiation, and proliferation; B cell activation; NK cell-mediated cytotoxicity; cell-cell adhesion; and TNF signaling, amongst others (Fig. 3c and Supplementary Table S7).

The strongest observed protein association with LAVi was that of known HF biomarker, N-terminal pro-B type natriuretic peptide (NT-proBNP). On average, LAVi was 3.09 mL/m² higher (11% of mean LAVi) per SD increment in plasma NT-proBNP (95% CI: 2.16–4.03; $FDR = 7.75 \times 10^{-9}$). Notably, among the top 5 strongest associations with LAVi was CRTAM, which also had the strongest association with HIV serostatus; LAVi was 2.37 mL/m² higher on average per SD (95% CI: 1.27–3.47; $FDR = 3.40 \times 10^{-4}$). The 73 proteins associated with LAVi exhibited pairwise correlations in plasma abundances that ranged widely from weak to strong (Supplementary Fig. S3) with several moderate confidence protein-protein interactions detected via STRING¹⁶ (Supplementary Fig. S4).

Next, we evaluated what proportion of the adjusted association between HIV and LAVi was accounted for by further adjustment for each identified proteome feature. When further adjusting the HIV-LAVi analysis for each of these 73 proteins separately (in addition to demographics, substance use, HCV, eGFR, and CVD risk factors), 38

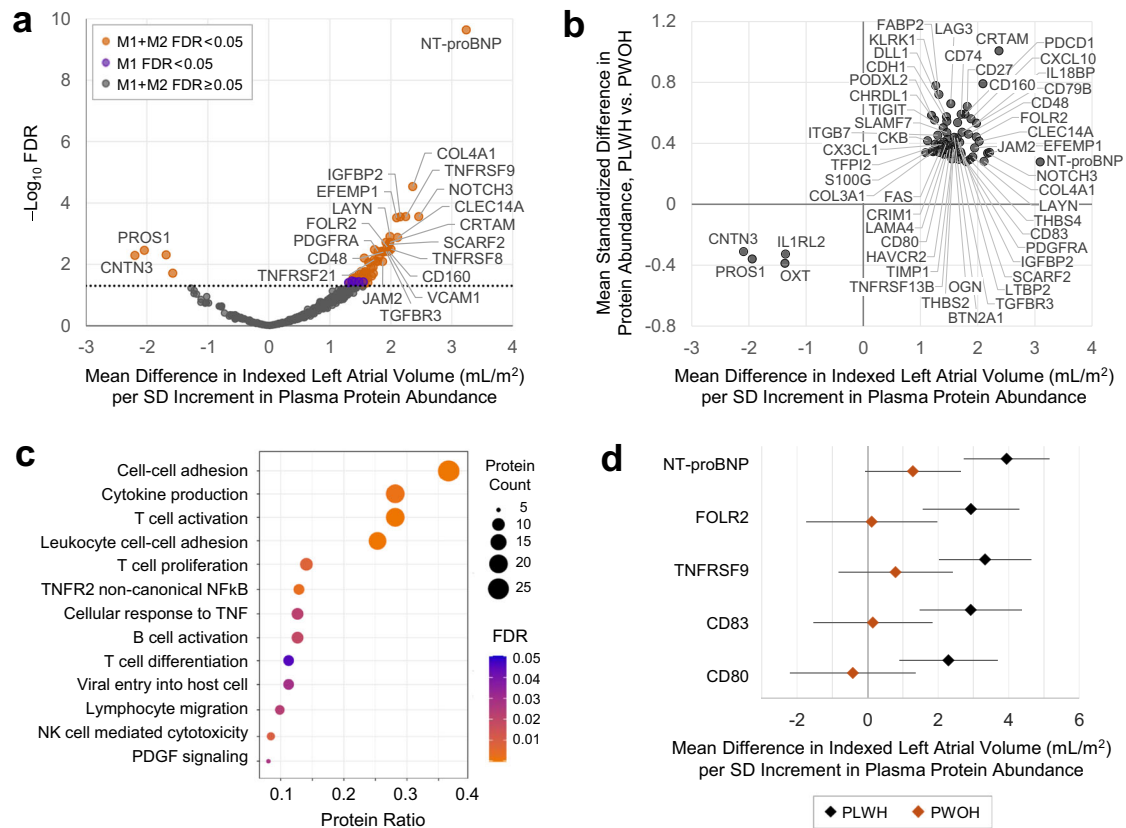


Fig. 3 | HIV-associated proteomic signature of left atrial size among people living with and without HIV in the United States ($n = 352$). **a** Volcano plot of mean differences in left atrial volume index (LAVi) per standard deviation (SD) increment in plasma abundance of 439 HIV-associated proteins vs. $-\log_{10}$ false discovery rate (FDR; Benjamini-Hochberg) estimated using linear regression with robust variance. Purple indicates proteins only associated in Model 1 (M1) when adjusting for sociodemographics, HIV, hepatitis C virus (HCV) infection, and renal function. Orange indicates proteins associated in Model 2 (M2) following further adjustment for education, cardiovascular risk factors, and substance use. The threshold for significance is indicated by a gray dotted line, $FDR < 0.05$. The most saturated model (orange) yielded 69 proteins positively associated with LAVi and 4 proteins inversely associated. Complete modeling results can be found in Supplementary Data 3. **b** Beta-beta plot of mean differences in standardized protein abundances comparing persons living with vs. without HIV (PLWH, PWOH) vs. mean differences in LAVi per SD increment in plasma protein abundances. All associations were estimated using linear regression with robust variance, and proteins depicted ($n = 73$) are restricted to those significantly associated with both

parameters with an $FDR < 0.05$. HIV point estimates (y-axis) were adjusted for sociodemographics, substance use, HCV, and renal function. LAVi point estimates (x-axis) were adjusted for the same covariates, plus HIV and cardiovascular risk factors. **c** Enriched biological processes among proteins associated with both positive HIV serostatus and higher LAVi (concordant directionality), estimated using a two-sided Fisher's exact test, Gene Ontology: Biological Processes annotations, and a threshold for significance of $FDR < 0.05$. Protein ratio = proportion of total signature proteins ($n = 73$) that map to the given annotation. TNF = tumor necrosis factor; NK = natural killer; PDGF = platelet-derived growth factor. Proteins mapping to each annotation can be found in Supplementary Table S7. **d** Mean differences in LAVi per SD increment in plasma protein abundances among strata of PLWH and PWOH, estimated using linear regression with robust variance adjusting for sociodemographics, substance use, cardiovascular risk factors, HCV, and renal function. Proteins depicted are limited to those with HIV \times protein multiplicative interactions with an $FDR < 0.10$ ($n = 73$ proteins tested). Error bars indicate 95% confidence intervals.

proteins reduced the adjusted HIV association by $>30\%$, and 8 reduced it by $>50\%$ —CRTAM, CD27, CD79B, CD160, TNF receptor superfamily (TNFRSF) 8, TNFRSF9, TNFRSF17, and IL18BP (Supplementary Table S8). Notably, adjustment for CRTAM reduced the association between positive HIV serostatus and higher LAVi by 82%, suggesting it may substantially account for that association.

We evaluated these 73 proteins for differences in adjusted LAVi associations by HIV serostatus and found no significant protein \times HIV interactions ($FDR < 0.05$). Given type II error is likely high for these multiplicative tests, we present interactions with higher significance thresholds to broaden hypothesis-generating potential. Five proteins exhibited associations with LAVi that differed by HIV serostatus at $FDR < 0.10$ and were present only among PLWH: NT-proBNP; CD80, CD83, and TNFRSF9 (CD137), all important immune checkpoint co-stimulatory molecules^{17–19}; and folate receptor β (FOLR2), an important folate binding protein expressed by myeloid cells, including infiltrating M2-like

macrophages²⁰ (Fig. 3d). See Supplementary Table S9 for complete results of individual protein interaction tests alongside modeling results stratified by HIV serostatus. We detected no protein \times age interactions (Supplementary Table S10).

In our multi-analyte approach, we found higher plasma level of the one agnostically defined HIV-associated protein cluster (Brown) was also associated with higher LAVi, adjusting for age, sex, race, ethnicity, eGFR, HCV, and HIV serostatus (2.03 mL/m² higher per SD increment in Brown cluster plasma level, 95% CI: 0.85–3.21; $p = 0.001$). Following further adjustment for substance use, education, and traditional CVD risk factors, the estimate of association was only mildly attenuated (1.96 mL/m² higher per SD, 95% CI: 0.75–3.16; $p = 0.002$, Fig. 4). We found adjustment for this protein cluster reduced the independent association between positive HIV serostatus and higher LAVi by 36%. Moreover, this association differed by HIV serostatus ($p = 0.006$) and was only present among PLWH. We did not detect an interaction with age ($p = 0.18$).

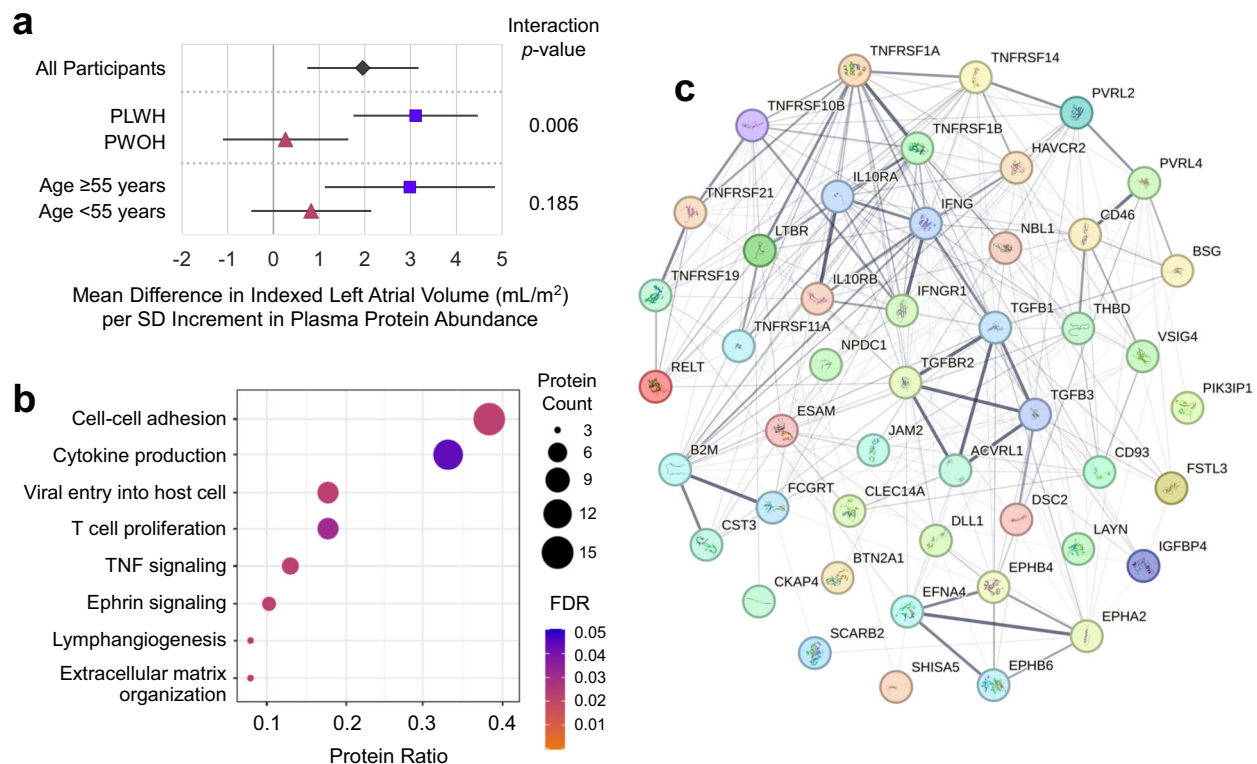


Fig. 4 | Relationship between an HIV-associated, agnostically defined cluster of plasma proteins and left atrial size among people living with and without HIV in the United States ($n = 352$). **a** Mean difference in indexed left atrial volume (LAVi) per standard deviation (SD) increment in ‘Brown’ protein cluster plasma abundance among all participants, among strata of participants living with and without HIV, and among strata of participants above and below median age in SMASH (55 years), estimated using linear regression with robust variance adjusting for sociodemographics, substance use, cardiovascular risk factors, hepatitis C virus infection, and renal function. Error bars indicate 95% confidence intervals. **b** Enriched biological processes among 42 proteins comprising the ‘Brown’ protein cluster, estimated using a two-sided Fisher’s exact test, Gene Ontology: Biological Processes annotations, and a threshold for significance of Benjamini-Hochberg

false discovery rate (FDR) < 0.05. Protein ratio = proportion of total ‘Brown’ cluster proteins ($n = 42$) that map to the given annotation. Proteins mapping to each annotation can be found in Supplementary Table S6. **c** Interaction network of 42 proteins comprising the ‘Brown’ protein cluster generated using STRING, a public database of known and predicted protein-protein interactions. Interactions include direct (physical) and indirect (functional) associations derived from computational prediction, knowledge transfer between organisms, and interactions aggregated from other databases. Line thickness indicates the strength of data support. Szklarczyk D, et al. The STRING database in 2023: protein-protein association networks and functional enrichment analyses for any sequenced genome of interest. *Nucleic Acids Res.* 2023;51(D1):D638-64.

We identified eleven proteins in both single- and multi-analyte approaches—specifically butyrophilin subfamily 2 member A1 (BTN2A1), C-type lectin domain containing 14 A (CLEC14A), delta-like canonical Notch ligand 1 (DLL1), ephrin A2 (EPHA2), endothelial cell adhesion molecule (ESAM), T cell immunoglobulin and mucin-domain containing-3 (TIM-3 or HAVCR2), junctional adhesion molecule 2 (JAM2), layilin (LAYN), TNFRSF1B, TNFRSF14, and TNFRSF21.

Associations between proteomic signature and clinical variables in SMASH

Many components of the identified protein signature were associated with age ($p < 0.05$), including the Brown cluster and 26 of 73 individual proteins. Notably, higher plasma CRTAM was not associated with traditional CVD risk factors (age, body mass index [BMI], hypertension, dyslipidemia, diabetes) but was associated with substance use (smoking and stimulant use) and many HIV-related factors (HCV, detectable plasma HIV RNA, lower current and nadir CD4 + T cell counts, not receiving ART and shorter ART duration). Similarly, the Brown protein cluster was largely only associated with substance use and HIV-related clinical factors—smoking, opioid use, HCV, detectable plasma HIV RNA, and lower current and nadir CD4 + T cell counts. See Supplementary Fig. S5 for the results of all evaluated protein associations with demographic and clinical characteristics.

External validation of protein signatures with indexed left atrial volume in MESA

A total of 1242 MESA participants had both CMR imaging and Olink Explore 3072 proteomic data (Supplementary Fig. S6), demographic and clinical characteristics of whom are summarized in Table 2. Participants were mean (SD) age 67 (9) years, 52% female, and had predominantly normal LVEF.

We tested each feature of the HIV-associated proteomic signature of LA remodeling that we identified in SMASH for associations with LAVi in MESA. Among these older PWOH, 8 of 73 plasma proteins were cross-sectionally associated with LAVi following multivariable adjustment (Table 3 and Supplementary Table S11). Following NT-proBNP, the strongest validated association was that of CLEC14A (mean difference: 1.36 mL/m² higher per SD, 95% CI: 0.65–2.07; FDR = 0.006), followed by collagen type IV alpha 1 chain (COL4A1) (1.20 mL/m² higher per SD, 95% CI: 0.56–1.85; FDR = 0.006). Moreover, 28 (of 73 proteins) had LAVi associations that differed by age (interaction FDR < 0.05, 41 proteins FDR < 0.10) (Supplementary Table S12); 16 of these were significant associations with LAVi only among a subgroup of MESA participants older than the median age at exam 5 (≥ 67 years), and only one (NT-proBNP) was associated among participants age < 67 years (Table 3). Furthermore, plasma level of the Brown protein cluster was associated with LAVi only among older MESA participants (age \geq

67 years, mean difference in LAVi per SD: 1.23 mL/m², 95% CI: 0.03–2.43; $p = 0.04$; age < 67 years: -0.72, 95% CI: -1.75–0.32; $p = 0.17$; interaction $p = 0.005$).

Table 2 | MESA external validation participant characteristics (exam 5, 2010–2012)

CHARACTERISTIC	Median [IQR] or % (n)	
	Cross-Sectional LAVi Analysis (n = 1242)	Incident Event Analysis (n = 2273)
Demographics		
Age, years	67 [60,74]	67 [61,75]
Female sex at birth	641 (52%)	1182 (52%)
Race and ethnicity		
Black, non-Hispanic	282 (23%)	550 (24%)
White, non-Hispanic	546 (44%)	950 (42%)
Hispanic	230 (18%)	444 (19%)
Chinese	184 (15%)	329 (15%)
Education level ≥ high school	1105 (89%)	2002 (88%)
Clinical Factors		
Smoking status		
Current	82 (7%)	156 (7%)
Former	540 (44%)	1016 (45%)
Never	620 (50%)	1101 (48%)
Pack-years of smoking	0 [0, 11]	0 [0, 12]
Body mass index, kg/m ²	27.3 [24.3, 30.7]	27.5 [24.4, 31.3]
Hypertension ^a	665 (54%)	1251 (55%)
Systolic blood pressure, mmHg	119 [108, 135]	119 [109, 136]
Diastolic blood pressure, mmHg	69 [62,75]	69 [62,75]
Blood pressure-lowering medication use	622 (50%)	1157 (51%)
Dyslipidemia ^b		
Total cholesterol, mg/dL	183 [159, 208]	182 [158, 208]
HDL-cholesterol, mg/dL	53 [44,63]	53 [44,64]
Lipid-lowering medication use	454 (37%)	865 (38%)
Diabetes ^c	236 (19%)	466 (21%)
Diabetes medication use	15 (13%)	29 (12%)
eGFR, CKD-EPI, mL/min/1.73m ²	84 [71,94]	83 [70,94]
Cardiovascular Magnetic Resonance		
LV ejection fraction, %	62.7 [58.1, 66.9]	–
LV ejection fraction < 50%	41 (3%)	–
LV mass indexed by BSA, mg/m ²	64.2 [56.3, 73.7]	–
LV end-diastolic volume indexed by BSA, mL/m ²	65.0 [57.1, 73.2]	–
LA volume indexed by BSA, mL/m ²	33.8 [27.2, 41.1]	–
LA volume indexed by BSA ≥ 40 mL/m ²	357 (29%)	–
LA volume indexed by BSA ≥ 53 mL/m ²	75 (6%)	–
Late gadolinium enhancement ^d	70 (9%)	–
Extracellular volume fraction, % ^e	26.8 [24.6, 29.0]	–

^a Hypertension is defined as the use of antihypertensive medications or systolic blood pressure ≥ 140 mmHg or diastolic blood pressure ≥ 90 mmHg.

^b Dyslipidemia is defined as the use of lipid-lowering medications or fasting total cholesterol level ≥ 200 mg/dL or low-density lipoprotein cholesterol level ≥ 130 mg/dL or high-density lipoprotein cholesterol level < 40 mg/dL or serum triglyceride level ≥ 150 mg/dL.

^c Diabetes is defined as use of hypoglycemic medication or fasting serum glucose levels ≥ 126 mg/dL.

^d Measured in a subgroup who received late gadolinium enhancement (n = 762).

^e Assessed in a subgroup who received T1 mapping (n = 258).

IQR=interquartile range, reported as [25th, 75th] percentiles; LV=left ventricular; LA=left atrial; BSA=body surface area; HDL=high-density lipoprotein; eGFR=estimated glomerular filtration rate.

External validation of protein signatures with incident clinical events in MESA

Incident clinical event analyses did not require CMR data and were performed in a larger subgroup of the MESA cohort to maximize statistical power (Supplementary Fig. S7). Distributions of demographic and clinical characteristics were similar to those in cross-sectional analyses presented above (Table 2).

Among 2185 MESA participants without known AF at exam 5, there were 252 incident AF events over a median [IQR] follow-up of 7.8 [0.9] years. Following multivariable adjustment, only NT-proBNP (of 73 proteins) was associated with time to incident AF (Supplementary Table S13 and Supplementary Fig. S8) (hazard ratio, HR: 1.54 per SD increment in NT-proBNP, 95% CI: 1.33–1.77; FDR = 2.08×10^{-7}). Plasma abundance of the Brown protein cluster was also associated with incident AF (HR: 1.18 per SD increment, 95%CI: 1.01 to 1.37; $p = 0.036$). No interactions with baseline age were detected (all FDR > 0.10).

Among 2273 MESA participants without known HF at exam 5, there were 54 incident adjudicated clinical HF events over a median [IQR] follow-up of 8.9 [0.8] years. Thirty of 73 proteins were associated with incident HF (Fig. 5), the strongest of which was TNFRSF1B (HR: 1.81 per SD increment, 95% CI: 1.41–2.33; FDR = 2.58×10^{-4}). Five of these proteins were also associated with LAVi in MESA when restricting to participants above the median age—CLEC14A, cysteine-rich transmembrane BMP regulator 1 (CRIM1), NT-proBNP, thrombospondin-2 (THBS2), and tissue inhibitor matrix metalloproteinase-1 (TIMP1). See Supplementary Table S14 for complete results of evaluated protein associations with time to incident HF. The hazard of HF was also significantly greater with higher plasma levels of the Brown protein cluster (HR: 1.79 per SD, 95% CI: 1.32 to 2.43; $p = 1.82 \times 10^{-4}$). No interactions with age were detected (all FDR > 0.10). Notably, 9 of 11 proteins identified in both single- and multi-analyte discovery analyses in SMASH were associated with incident HF in MESA—BTN2A1, CLEC14A, DLL1, ESAM, HAVCR2, JAM2, LAYN, TNFRSF1B, and TNFRSF14.

Associations between validated proteomic signature features and clinical variables

Each component of the protein signature validated with clinical HF among MESA participants was positively and strongly associated with older age (all $p < 0.001$) (Supplementary Fig. S9). All identified proteome features were also strongly associated with lower eGFR, and many with hypertension (28 proteins and Brown cluster), diabetes (25 proteins and Brown cluster), and higher BMI (22 proteins and Brown cluster)—which remained associated following adjustment for eGFR.

Discussion

In this discovery study, we identified a distinct plasma proteomic signature of left atrial remodeling—a marker of subclinical heart disease—that was heightened among PLWH and was also strongly associated with age and higher risk for incident clinical HF among a large independent cohort of PWOH who were over 10 years older. This proteomic signature comprised 73 individual proteins and one agnostically-defined cluster of 42 proteins, largely comprising immune checkpoint proteins (ICPs), cytokine signaling, ephrin signaling, and ECM organization pathways. Our findings support the premise that persistent immune activation, higher systemic inflammation, and fibrosis are related to HIV-associated atrial remodeling, even among virally suppressed PLWH on ART, and some of these mechanisms may parallel those of aging-related HF among the general population.

It is well-known that PLWH exhibits elevated systemic inflammation and immune activation compared to PWOH, characterized by T cell exhaustion, macrophage activation, and elevated levels of circulating pro-inflammatory cytokines that persist even among virally suppressed PLWH on ART. Immunosenescence is a well-described

Table 3 | Summary of cross-sectional associations between identified HIV-associated proteomic signature of left atrial size and indexed left atrial volume by age among people without HIV in MESA (n = 1242)

Analysis Sample	Mean (SD) Age	Proteins FDR < 0.05 ^a
All participants	68 (9)	CKB, CLEC14A , CNTN3, COL4A1 , IGFBP2, NOTCH3 , NT-proBNP, PDGFRA
Participants ≥ median age	75 (5)	B3GNT7 , CLEC14A , COL4A1 , CRIM1 , CX3CL1 , DCTPP1 , EPHA2 , LTBP2 , NOTCH3 , NT-proBNP, PDGFRA, SCARF2 , THBS2 , THBS4 , TIMP1 , VCAM1 , Brown protein cluster
Participants < median age	60 (4)	NT-proBNP

^a Estimated using linear regression with robust variance, adjusting for field center, sociodemographics, smoking, cardiovascular risk factors, and renal function.

Bold indicates protein × continuous age interaction with an FDR < 0.05 evaluated at exam 5 (2010–2012, median age 67 years). Brown protein cluster comprises 42 proteins and is described in Fig. 3. Complete modeling results can be found in Supplementary Tables S11 and S12.

consequence of aging, and maladaptively activated innate and adaptive immune responses have also been implicated in acute and chronic HF²¹. This is the prevailing hypothesized mechanism through which PLWH experiences excess risk of aging-related diseases, including HF, and our findings support and expand upon those previously put forward.

We identified 30 proteins associated with HIV serostatus and LAVi in SMASH as well as incident clinical HF among older PWOH in MESA. Five of these proteins were associated with LAVi among PWOH in MESA when restricting to participants above median age. Interestingly, this list also included several proteins exhibiting especially high potential for mediating and/or moderating effects on the association between HIV and atrial remodeling and also included 9 proteins identified in both single- and multi-analyte discovery analyses. This overlap in identification is important because these approaches are both agnostic and independent of each other; identification by both approaches therefore strengthens the plausibility of the identified proteins as potential contributors to or biomarkers of both HIV- and aging-related LA remodeling and HF.

Many of these proteins of especially high interest are important ICPs—specifically CD27, TNFRSF8 (CD30), CD79B, CD80, TNFRSF9 (CD137), HAVCR2 (TIM-3), TNFRSF14 (HVEM), TIGIT, TNFRSF1B (TNFR2), and less extensively studied BTN2A1, CD83, IL18BP, and TNFRSF17. Many of the remaining proteins—CLEC14A, CRIM1, DLL1, ESAM, JAM2, LAYN, THBS2, and TIMP1—are involved broadly in cell migration and tissue homeostasis.

Activation of T cells, B cells, and NK cells is regulated by several costimulatory and inhibitory ICPs. Elevated expression of ICPs is a known consequence of HIV infection that persists despite ART-induced viral suppression and contributes to immune dysfunction, HIV disease progression, and viral persistence²². Many ICPs we identified belong to the TNF receptor superfamily, the upregulation of which is both a hallmark of HIV-associated inflammation and immune activation²³ and has been extensively observed in HF²⁴. Higher soluble CD27 and CD80 have also recently been identified as correlates of risk for non-AIDS adverse events among PLWH receiving ART²⁵. Therapeutic blockade of ICPs has, however, proven controversial and effects are dependent on whether target molecules serve costimulatory or co-inhibitory functions. Taken together with the unique features of HIV-associated immune dysfunction, these findings highlight the need for focused future investigation of ICPs in HIV-associated cardiac remodeling and HF.

In this study, the one agnostically defined protein cluster of interest included four proteins involved in ephrin signaling, one of which was also identified in single-analyte discovery analyses (EPHA2). Ephrin signaling mediates a wide range of cellular processes involved in tissue homeostasis and response to injury, including angiogenesis and activation/migration of T cells, B cells, and macrophages²⁶. Though not well-studied among PLWH, ephrin signaling has been linked to other viral infections²⁷ as well as cardiomyocyte development, systolic and diastolic function, and TGF-β mediated cardiac fibrosis^{28–30}.

Several of these higher-interest proteins are related to tissue growth and development, angiogenesis, and ECM remodeling—

including CRIM1, THBS2, and TIMP1. CRIM1 modulates the activity of bone morphogenic proteins, members of the TGFβ superfamily that are known to play roles in cardiac development and disease pathophysiology in HF, pulmonary arterial hypertension, and atherosclerosis³¹. Both THBS2 and TIMP1 are critical regulators of tissue homeostasis with roles in ECM remodeling, angiogenesis, and cell growth/differentiation, and have been extensively implicated in HF pathogenesis^{32,33}, including in recent plasma proteome studies^{34–36}.

Other high-interest proteome features have been linked to the migration of various immune cell subsets in tissue homeostasis—specifically DLL1 (a ligand of Notch receptors), ESAM (endothelial cell adhesion molecule), JAM2 (involved in cell migration), and LAYN (involved in focal adhesion). Immune cell recruitment plays an important role in myocardial response to injury²¹; however, further investigation is needed to clarify the role of these proteins in shared mechanisms of HIV- and aging-related cardiac remodeling and HF.

Few proteins were inversely associated with positive HIV serostatus and higher LAVi in SMASH. One of these four proteins—contactin-3 (CNTN3)—was validated in its inverse association with LAVi among all MESA participants, though it was not associated with time to incident AF or HF. There is evidence from murine models that CNTN3 may be associated with aging, inflammation, and vascular permeability³⁷, and a protective effect of a closely related contactin (CNTN1) was recently identified in a proteomics study of incident HF³⁴.

We identified potential biological contributors to the association between HIV and LA remodeling. The abundance of one protein—CRTAM—reduced that association by 82%, markedly more than any other protein, and was strongly associated with several clinical factors related to HIV disease severity. CRTAM is an immune activation marker expressed by NK cells, CD8 + T cells, and a subset of CD4 + T cells with enhanced cytotoxic activity³⁸. Measures of CRTAM expression have previously been associated with positive HIV serostatus, HIV viral reservoir size, and viral rebound kinetics^{39,40}. CRTAM is also believed critical to shaping the gut microbiome and Th17 responses at the mucosa⁴¹, increased permeability of which is a consequence of Th17 HIV-susceptibility and a contributor to chronic inflammation among PLWH⁴². CRTAM was not associated with LAVi or incident HF among older PWOH in MESA, consistent with the hypothesis that it may be an HIV-specific biomarker of CVD. Taken together, our results and prior work suggest CRTAM may represent an HIV-specific marker of cardiovascular risk worthy of further investigation into its prognostic and therapeutic utility.

There are limitations to this study. Protein levels measured with Olink are semi-quantitative, limiting comparison to other assays. Previously published data demonstrated many proteins assessed by Olink Explore 3072 were associated with cis-protein quantitative trait loci (pQTLs), suggesting specificity of protein identification⁴³. Nonetheless, all proteins of interest require validation using other methods. Type II error may be inflated due to the method used for multiple testing correction, which assumes independence of tests (i.e., biological independence of proteins) and is therefore conservative. For example, given macrophage activation is a hallmark of chronic immune

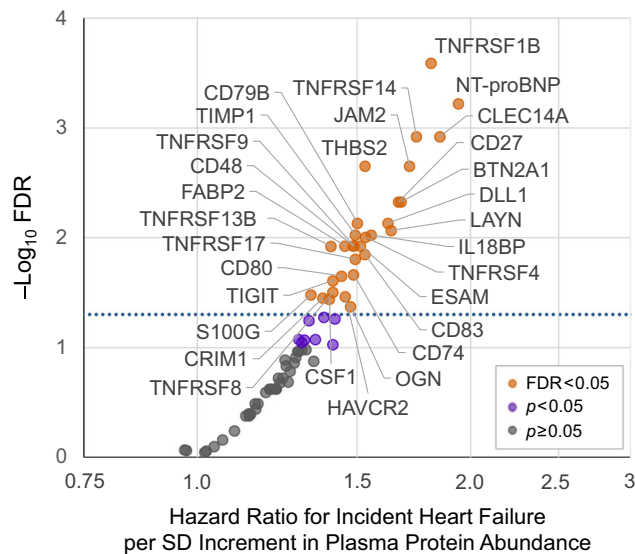


Fig. 5 | Associations between identified HIV-associated proteomic signature of left atrial size and time to incident adjudicated clinical heart failure in the Multi-Ethnic Study of Atherosclerosis ($n = 2273$). Hazard ratios were estimated using Cox proportional hazards adjusting for study site, age, sex, race, ethnicity, educational attainment, body mass index, systolic blood pressure, anti-hypertensive medication, dyslipidemia, diabetes, smoking, and estimated glomerular filtration rate. $N = 54$ incident adjudicated heart failure events. Purple indicates $p < 0.05$, Orange indicates $FDR < 0.05$. Complete modeling results can be found in Supplementary Table S14, and source data are provided as a Source Data file. SD = standard deviation; FDR = false discovery rate (Benjamini-Hochberg).

activation among PLWH, we hypothesized it would be detected in our enrichment analyses. It was indeed positively associated with HIV and LAVi in SMASH but not following multiple testing corrections ($p = 0.03$; $FDR = 0.36$). Type II error may be of particular concern in analyses among subpopulations or involving multiplicative interactions. Discovery analyses are cross-sectional and lacking incident event data, resulting in temporal ambiguity. There are also limitations of incident event ascertainment in MESA, particularly for AF which relied on hospitalizations and claims data alone, possibly leading to misclassification bias. Finally, though we believe it strengthens the validity of our detected associations, discovery and external study populations substantially differ demographically, sociobehaviorally, and clinically (e.g., prevalence of HIV and HCV infection). We were therefore unable to externally evaluate the identified proteomic signature of HIV serostatus. In addition, though observed associations with LAVi in SMASH discovery analyses were independent of HIV serostatus and other major factors that differed between populations (e.g., substance use, age, sex), it cannot be discounted that unvalidated proteins may simply be more clinically relevant among the source population represented in SMASH.

In conclusion, we discovered a plasma proteomic signature that may in part reflect or contribute to HIV-associated left atrial remodeling and also predicted incident clinical heart failure, as evidenced among a large independent cohort of older people without HIV. This signature was enriched in pathways of immune activation, cytokine signaling, and extracellular matrix organization. Our findings suggest some pathways underlying the risk of heart failure among people with HIV may also contribute to heart failure pathogenesis among older people without HIV. If successfully validated in other external populations, these proteins may help refine current risk prediction models and help identify therapeutic targets for heart failure among both people with and without HIV.

Methods

Discovery study population (SMASH)

Participants in the SMASH study were recruited from the Multicenter AIDS Cohort Study (MACS), the Women's Interagency HIV Study (WIHS), and the AIDS Linked to the Intravenous Experience (ALIVE) study and underwent CMR with concurrent blood collection and storage between March 2015 and February 2018 under a single, centralized protocol. All three cohorts include PLWH and PWOH. The WIHS and MACS are multicenter observational longitudinal cohort studies composed of women or men who have sex with men, respectively^{44,45}. The ALIVE study is a community-based cohort of men and women with a history of injection drug use⁴⁶. By leveraging three well-established cohorts with distinct source populations for enrollment, we recruited participants into SMASH with diverse sociodemographic and HIV-related risk factors, highly representative of people with and at risk of HIV in the United States. See the Supplementary Information for additional cohort details. The SMASH study enrolled active participants 40–70 years of age from the Chicago and Baltimore/Washington, DC MACS sites, the Washington, DC WIHS site; and the ALIVE study, which is based in Baltimore. Exclusion criteria included eGFR (Chronic Kidney Disease Epidemiology Collaboration 2021) < 45 mL/min/1.73 m², weight > 350 pounds, known claustrophobia or contrast allergy, and contraindications to CMR. Proteomics was performed on a subset of total SMASH participants with complete CMR and adequate stored plasma volume (Supplementary Fig. S1). All participants provided informed consent. This study conforms to the ethical principles of the Declaration of Helsinki and has been approved by the Institutional Review Boards of Johns Hopkins University, Georgetown University, and Northwestern University.

Sociobehavioral and clinical data in SMASH

Participants completed an interviewer-administered structured questionnaire and biological measures concurrent with CMR. Prescribed medications, history of CVD, and substance use during the preceding 5 years were queried. These data were supplemented with data collected through the MACS, WIHS, and ALIVE cohorts, including self-reported demographics and CVD risk factors. See Supplementary Information for a full list and definitions of covariates. Among PLWH, measures of HIV disease activity included current plasma HIV RNA concentrations (Roche ultrasensitive assay), current and nadir CD4+ T cell counts/ μ L, history of AIDS-defining malignancy or opportunistic infection, and use of ART, including regimen type.

Cardiovascular magnetic resonance in SMASH

CMR was performed at Johns Hopkins Hospital (Baltimore) or Northwestern Memorial Hospital (Chicago) on 1.5 T Siemens Avanto or Aera scanners (Erlangen, Germany) using a standardized protocol that included gadolinium enhancement, detailed in the Supplementary Information. Briefly, short and long-axis cines (30 phases/cardiac cycle) were acquired with a steady-state free precession sequence. Multimodality Tissue Tracking software (MTT; version 6.0, Toshiba, Japan) was used to quantify LA volumes and other standard metrics⁴⁷, blinded to participant characteristics. Maximum LA volume was measured using the LA volume curve generated by the Simpson's method from four-chamber and two-chamber views and was indexed to body surface area (LAVi).

Proteomics in SMASH

We performed proteomics on EDTA plasma stored at -80 °C using the Olink Explore 3072 platform at the Laboratory of Clinical Investigation at the National Institute on Aging, NIH (Baltimore, MD) using a standardized protocol. Olink technology employs DNA oligonucleotide-

labeled antibody pairs that bind target antigens in solution and, when bound pairwise, hybridize and are extended by a DNA polymerase. This forms a DNA barcode, which is then amplified and quantified by microfluidic quantitative PCR⁴⁸. Additional details are outlined in the Supplementary Information alongside data quality control, normalization, and calibration procedures. Values are reported as log₂-transformed relative plasma abundances, which were winsorized to 5 SD to minimize the effect of outliers (median: zero observations winsorized per protein; range: 0.00% to 0.13%) and standardized for comparability. Following quality control, no samples were excluded, and 2594 proteins were analyzed with final mean intra- and inter-assay coefficients of variation of 9% and 15%, respectively.

Weighted gene co-expression network analysis

High-dimensional proteomic data often contain informative patterns lost when analyzing proteins individually. To address this, we derived unique clusters of highly correlated proteins using weighted gene co-expression network analysis implementing the R 'WGCNA' package (version 1.72). See Supplementary Information for details.

Statistical modeling

A graphical representation of the study design and analytic flow is depicted in Fig. 1. Complete case analyses were performed to estimate cross-sectional associations between plasma protein abundances and both HIV serostatus and continuous LAVi. Proteins were analyzed individually (single-analyte approach) and as clusters agnostically defined using WGCNA (multi-analyte approach). Inference was made using multivariable linear regression with Huber-White robust variance estimators to account for likely heteroscedasticity. Analyses were corrected for multiple comparisons using a step-down false discovery rate procedure defined by Benjamini and Hochberg and a two-sided threshold for significance of FDR < 0.05.

Mean standardized differences in plasma protein abundances by HIV serostatus were first estimated by adjusting for age, sex, race/ethnicity, educational attainment (dichotomized at high school diploma), current hazardous alcohol use, pack-years of smoking in prior 5 years, stimulant use in prior 5 years, opioid use in prior 5 years, HCV, and eGFR. Mean differences in LAVi were then estimated per SD increment in individual plasma protein abundances, restricting to proteins with HIV associations (at FDR < 0.05) and adjusting for covariates above, and for HIV serostatus, BMI, systolic blood pressure (SBP), hypertension medication use, dyslipidemia, and diabetes. The study site was not adjusted for in these analyses due to collinearity with sex. Proteins of interest were defined as those with significant adjusted associations with both HIV serostatus and LAVi. Given known biological differences among PLWH with vs. without viral suppression on ART, we further analyzed proteome features in subgroup analyses excluding PLWH with detectable HIV RNA (> 50 copies/mL) to evaluate their relevance in the context of successful HIV viremic control. We assessed the degree to which they may reflect the association between positive HIV serostatus and higher LAVi. We evaluated differences in their associations with LAVi by HIV serostatus and age using multiplicative interaction terms. We estimated protein associations with basic clinical and HIV-related characteristics.

Functional annotation analysis

Annotation-based overrepresentation analyses were performed using the Gene Ontology (GO): Biological Processes annotation database and the R 'clusterProfiler' package (version 4.6)⁴⁹. This employs a Fisher's exact test comparing the proportion of significantly associated proteins mapping to a given functional annotation to the proportion of total analyzed proteins mapping to the same annotation. The background used in these analyses was proteins measured on Olink Explore

3072 that passed quality control. Relationships between proteins of interest were further explored using interaction networks generated using a database of known and predicted protein-protein interactions, STRING¹⁶.

External validation cohort (older persons without HIV in MESA)

External validation was performed in MESA, a prospective community-based cohort initiated in 2000 to study the characteristics and progression of subclinical CVD among a diverse population in the United States, age 45–84 years without clinical CVD at baseline⁵⁰. We used data from exam 5 (years 2010–2012) when participants were aged 53–94 years due to the use of the same CMR protocol⁵¹ and proteomics platform (Olink Explore 3072) as SMASH at that time point. MESA participants were also, on average, over 10 years older than SMASH participants at exam 5, allowing a more extensive evaluation of the impact of older age on the identified proteomic signature among PWOH. See Supplementary Information for the study population and data acquisition details.

We first performed cross-sectional analyses of LAVi among MESA participants with proteomics and CMR using the same statistical modeling approach as described above, with slight variation in covariates due to differences in data collection or prevalences among study populations—specifically, we adjusted for field center, age, sex, race/ethnicity, education level, smoking, BMI, SBP, blood pressure-lowering therapy, dyslipidemia, diabetes, and eGFR.

We additionally assessed associations of identified proteomic signatures with time to incident AF and incident clinical HF. AF was defined by the presence of ≥1 inpatient or outpatient International Classification of Diseases, Ninth Revision codes for AF. HF criteria included symptomatic, physician-diagnosed HF as well as ≥1 of the following: (i) pulmonary edema/congestion by chest x-ray; (ii) dilated LV or poor LV function by echocardiography or ventriculography; and/or (iii) evidence of LV diastolic dysfunction. Inpatient and/or outpatient records were independently reviewed by two physicians for HF classification and event date assignment. See Supplementary Information for detailed ascertainment and adjudication procedures. Hazard ratios were estimated per SD increment in plasma protein level using Cox proportional hazards models adjusting for the same covariates as cross-sectional analyses. Participants with prevalent disease (AF or HF) at the start of follow-up were excluded from those analyses, and time at risk was calculated as the time from the date of MESA exam 5 to the incident event, death, loss to follow-up, or end of follow-up, whichever occurred first.

Lastly, we estimated associations between proteins validated with at least one outcome and basic clinical characteristics adjusted for field centers. All analyses were conducted using R (version 4.2).

Reporting summary

Further information on research design is available in the Nature Portfolio Reporting Summary linked to this article.

Data availability

The processed data generated in this study are available in the Supplementary Information and Source Data file provided with this manuscript. Anonymized individual-level SMASH and MESA data access procedures are in accordance with participant informed consent and NIH data sharing policies. Given the sensitive nature of data collected in SMASH, requests for data sharing from researchers certified in human subject confidentiality can be submitted to and will be reviewed by the parent cohorts according to established study procedures: <https://statepi.jhsph.edu/mwccs/> and <https://www.jhsph.edu/research/affiliated-programs/aids-linked-to-the-intravenous-experience/>. MESA data are available upon request through BioLINCC (<https://biolincc.nhlbi.nih.gov/studies/mesa/>) according to

established study procedures, and MESA proteomics data, generated as part of the NHLBI Trans-Omics for Precision Medicine (TOPMed) program, are available via the NHLBI database of Genotypes and Phenotypes (dbGaP, accession number: phs001416.v3.p1 NHLBI TOPMed: MESA and MESA Family AA-CAC). Source data are provided in this paper.

Code availability

Only publicly available statistical packages were used in the analyses of this study, detailed in Statistical Methods. The code and further details on employed packages are available from the corresponding author upon request.

References

1. Feinstein, M. J. et al. Characteristics, prevention, and management of cardiovascular disease in people living with HIV: A scientific statement from the American Heart Association. *Circulation* **140**, e98–e124 (2019).
2. Wu, K. C., Woldu, B., Post, W. S. & Hays, A. G. Prevention of heart failure, tachyarrhythmias and sudden cardiac death in HIV. *Curr. Opin. HIV AIDS* **17**, 261–269 (2022).
3. Alonso, A., Barnes, A. E., Guest, J. L., Shah, A., Shao, I. Y. & Marconi, V. HIV Infection and incidence of cardiovascular diseases: An analysis of a large healthcare database. *J. Am. Heart Assoc.* **8**, e012241 (2019).
4. Freiberg, M. S. et al. Association between HIV infection and the risk of heart failure with reduced ejection fraction and preserved ejection fraction in the antiretroviral therapy era: Results from the veterans aging cohort study. *JAMA Cardiol.* **2**, 536–546 (2017).
5. Chen, Y. et al. Human immunodeficiency virus infection and incident heart failure: A meta-analysis of prospective studies. *J. Acquir. Immune Defic. Syndr.* **87**, 741–749 (2021).
6. Sardana, M. et al. Human immunodeficiency virus infection and incident atrial fibrillation. *J. Am. Coll. Cardiol.* **74**, 1512–1514 (2019).
7. Sinha, A. & Feinstein, M. Epidemiology, pathophysiology, and prevention of heart failure in people with HIV. *Prog. Cardiovasc. Dis.* **63**, 134–141 (2020).
8. Doria de Vasconcellos, H. et al. Associations between HIV serostatus and cardiac structure and function evaluated by 2-dimensional echocardiography in the multicenter AIDS cohort study. *J. Am. Heart Assoc.* **10**, e019709 (2021).
9. Wu, K. C. et al. Human immunodeficiency viral infection and differences in interstitial ventricular fibrosis and left atrial size. *Eur. Heart J. Cardiovasc. Imaging* **22**, 888–895 (2021).
10. Hsue, P. Y. et al. Impact of HIV infection on diastolic function and left ventricular mass. *Circ. Heart Fail.* **3**, 132–139 (2010).
11. Reinsch, N. et al. Echocardiographic findings and abnormalities in HIV-infected patients: results from a large, prospective, multicenter HIV-heart study. *Am. J. Cardiovasc. Dis.* **1**, 176–184 (2011).
12. Shuldiner, S. R. et al. Myocardial fibrosis among antiretroviral therapy-treated persons with human immunodeficiency virus in South Africa. *Open Forum Infect. Dis.* **8**, ofaa600 (2021).
13. Zanni, M. V. et al. Immune correlates of diffuse myocardial fibrosis and diastolic dysfunction among aging women with human immunodeficiency virus. *J. Infect. Dis.* **221**, 1315–1320 (2020).
14. Nagueh, S. F. et al. Recommendations for the evaluation of left ventricular diastolic function by echocardiography: An update from the American society of echocardiography and the European association of cardiovascular imaging. *Eur. Heart J. Cardiovasc. Imaging* **17**, 1321–1360 (2016).
15. Peterson, T. E. et al. Circulating biomarker correlates of left atrial size and myocardial extracellular volume fraction among persons living with and without HIV. *BMC Cardiovasc. Disord.* **22**, 393 (2022).
16. Szklarczyk, D. et al. The STRING database in 2023: protein-protein association networks and functional enrichment analyses for any sequenced genome of interest. *Nucleic Acids Res.* **51**, D638–D646 (2023).
17. Simons, K. H., de Jong, A., Jukema, J. W., de Vries, M. R., Arens, R. & Quax, P. H. A. T cell co-stimulation and co-inhibition in cardiovascular disease: a double-edged sword. *Nat. Rev. Cardiol.* **16**, 325–343 (2019).
18. Yousif, L. I., Tanja, A. A., de Boer, R. A., Teske, A. J. & Meijers, W. C. The role of immune checkpoints in cardiovascular disease. *Front. Pharm.* **13**, 989431 (2022).
19. Grosche, L. et al. The CD83 molecule - An important immune checkpoint. *Front. Immunol.* **11**, 721 (2020).
20. Puig-Kröger, A. et al. Folate receptor beta is expressed by tumor-associated macrophages and constitutes a marker for M2 anti-inflammatory/regulatory macrophages. *Cancer Res.* **69**, 9395–9403 (2009).
21. Adamo, L., Rocha-Resende, C., Prabhu, S. D. & Mann, D. L. Reappraising the role of inflammation in heart failure. *Nat. Rev. Cardiol.* **17**, 269–285 (2020).
22. Gubser, C., Chiu, C., Lewin, S. R. & Rasmussen, T. A. Immune checkpoint blockade in HIV. *EBioMedicine* **76**, 103840 (2022).
23. Wang, C. & Watts, T. H. Maintaining the balance: costimulatory TNFRs and control of HIV. *Cytokine Growth Factor Rev.* **23**, 245–254 (2012).
24. Murphy, S. P., Kakkar, R., McCarthy, C. P. & Januzzi, J. L. Inflammation in heart failure: JACC state-of-the-art review. *J. Am. Coll. Cardiol.* **75**, 1324–1340 (2020).
25. Premeaux, T. A. et al. Monitoring circulating immune checkpoint proteins as predictors of non-AIDS morbid events in people with HIV initiating antiretroviral therapy. *Open Forum Infect. Dis.* **9**, ofab570 (2022).
26. Darling, T. K. & Lamb, T. J. Emerging roles for Eph receptors and Ephrin ligands in immunity. *Front. Immunol.* **10**, 1473 (2019).
27. de Boer, E. C. W., van Gils, J. M. & van Gils, M. J. Ephrin-Eph signaling usage by a variety of viruses. *Pharm. Res.* **159**, 105038 (2020).
28. Luxan, G. et al. Endothelial EphB4 maintains vascular integrity and transport function in adult heart. *Elife* **8**, <https://doi.org/10.7554/elife.45863> (2019).
29. Karsenty, C. et al. Ephrin-B1 regulates the adult diastolic function through a late postnatal maturation of cardiomyocyte surface crests. *Elife* **12**, <https://doi.org/10.7554/elife.80904> (2023).
30. Su, S. A., Xie, Y., Zhang, Y., Xi, Y., Cheng, J. & Xiang, M. Essential roles of EphrinB2 in mammalian heart: from development to diseases. *Cell Commun. Signal* **17**, 29 (2019).
31. Ye, D. et al. Insights into bone morphogenetic proteins in cardiovascular diseases. *Front. Pharm.* **14**, 1125642 (2023).
32. Zhang, K., Li, M., Yin, L., Fu, G. & Liu, Z. Role of thrombospondin-1 and thrombospondin-2 in cardiovascular diseases (Review). *Int. J. Mol. Med.* **45**, 1275–1293 (2020).
33. Moore, L., Fan, D., Basu, R., Kandalam, V. & Kassiri, Z. Tissue inhibitor of metalloproteinases (TIMPs) in heart failure. *Heart Fail. Rev.* **17**, 693–706 (2012).
34. Egerstedt, A. et al. Profiling of the plasma proteome across different stages of human heart failure. *Nat. Commun.* **10**, 5830 (2019).
35. Wells, Q. S. et al. Accelerating biomarker discovery through electronic health records, automated biobanking, and proteomics. *J. Am. Coll. Cardiol.* **73**, 2195–2205 (2019).
36. Regan, J. A. et al. Protein biomarkers of cardiac remodeling and inflammation associated with HFpEF and incident events. *Sci. Rep.* **12**, 20072 (2022).
37. Raza, A. et al. A natural mouse model reveals genetic determinants of systemic capillary leak syndrome (Clarkson disease). *Commun. Biol.* **2**, 398 (2019).

38. Hermans, D., van Beers, L. & Broux, B. Nectin family ligands trigger immune effector functions in health and autoimmunity. *Biology* **12**, <https://doi.org/10.3390/biology12030452> (2023).
39. Corley, M. J., Pang, A. P. S., Rasmussen, T. A., Tolstrup, M., Søgaard, O. S. & Ndhlovu, L. C. Candidate host epigenetic marks predictive for HIV reservoir size, responsiveness to latency reversal, and viral rebound. *AIDS* **35**, 2269–2279 (2021).
40. Sperk, M., Zhang, W., Nowak, P. & Neogi, U. Plasma soluble factor following two decades prolonged suppressive antiretroviral therapy in HIV-1-positive males: A cross-sectional study. *Medicine* **97**, e9759 (2018).
41. Perez-Lopez, A. et al. CRTAM Shapes the gut microbiota and enhances the severity of infection. *J. Immunol.* **203**, 532–543 (2019).
42. Renault, C. et al. Th17 CD4+ T-Cell as a preferential target for HIV reservoirs. *Front. Immunol.* **13**, 822576 (2022).
43. Eldjarn, G. H. et al. Large-scale plasma proteomics comparisons through genetics and disease associations. *Nature* **622**, 348–358 (2023).
44. Kaslow, R. A., Ostrow, D. G., Detels, R., Phair, J. P., Polk, B. F. & Rinaldo, C. R. The multicenter AIDS cohort study: rationale, organization, and selected characteristics of the participants. *Am. J. Epidemiol.* **126**, 310–318 (1987).
45. Barkan, S. E. et al. The women's interagency HIV study. WIHS collaborative study group. *Epidemiol.* **9**, 117–125 (1998).
46. Vlahov, D. et al. The ALIVE study, a longitudinal study of HIV-1 infection in intravenous drug users: description of methods and characteristics of participants. *NIDA Res. Monogr.* **109**, 75–100 (1991).
47. Tao, S. et al. Impaired left atrial function predicts inappropriate shocks in primary prevention implantable cardioverter-defibrillator candidates. *J. Cardiovasc. Electrophysiol.* **28**, 796–805 (2017).
48. Ebai, T., Kamali-Moghaddam, M. & Landegren, U. Parallel protein detection by solid-phase proximity ligation assay with real-time PCR or sequencing. *Curr. Protoc. Mol. Biol.* **109**, 20.10.21–20.10.25 (2015).
49. Wu, T. et al. clusterProfiler 4.0: A universal enrichment tool for interpreting omics data. *Innovation* **2**, 100141 (2021).
50. Bild, D. E. et al. Multi-ethnic study of atherosclerosis: objectives and design. *Am. J. Epidemiol.* **156**, 871–881 (2002).
51. Ambale-Venkatesh, B. et al. Left atrial remodeling assessed by serial longitudinal cardiac MRI in MESA. *JACC Cardiovasc. Imaging* **14**, 1678–1680 (2021).

Acknowledgements

This study was supported in part by the National Institutes of Health (NIH: R01 HL126552 (SMASH study, K.C.W. and W.S.P.); U01-DA036297 (ALIVE data collection); and U01-HL146201, U01-HL146193, U01-HL146240, and U01-HL146205 (MACS, WIHS data collection). Proteomics was supported by U01HL146201, Johns Hopkins University Center for AIDS Research (P30AI094189), the Intramural Research Program of the National Institute on Aging, NIH (ZIAAG000297), and Dr. Nancy Grasmick. Support for the Multi-Ethnic Study of Atherosclerosis (MESA) projects are conducted and supported by the National Heart, Lung, and Blood Institute (NHLBI) in collaboration with MESA investigators. Support for MESA is provided by contracts 75N92020D00001, HHSN2682015000031, N01-HC-95159, 75N92020D00005, N01-HC-95160, 75N92020D00002, N01-HC-95161, 75N92020D00003, N01-HC-95162, 75N92020D00006, N01-HC-95163, 75N92020D00004, N01-HC-95164, 75N92020D00007, N01-HC-95165, N01-HC-95166, N01-HC-95167, N01-HC-95168, N01-HC-95169, UL1-TR-000040, UL1-TR-001079, UL1-TR-001420, UL1TR001881, DK063491, and R01HL105756. Molecular data for the Trans-Omics in Precision Medicine (TOPMed) program was supported by the NHLBI. Proteomics was supported by TOPMed MESA Multi-Omics (HHSN2682015000031, HSN26800004, HHSN2682016000341).

Core support, including centralized genomic read mapping and genotype calling, along with variant quality metrics and filtering were provided by the TOPMed Informatics Research Center (3R01HL-117626-02S1; contract HHSN2682018000021). Core support, including phenotype harmonization, data management, sample-identity QC, and general program coordination, was provided by the TOPMed Data Coordinating Center (R01HL-120393; U01HL-120393; contract HHSN2682018000011). TEP is supported by NIH/NHLBI T32 HL007227. T.T.B. is supported in part by K24 AI120834. V.S.H. is supported by NIH NHLBI 1K23HL166770-01 and the Sarnoff Scholar Award 138828. The authors gratefully acknowledge the contributions of the study participants and the dedication of the MWCCS, ALIVE, SMASH, and MESA-TOPMed investigators and staff. Full MWCCS acknowledgement may be found at <https://statepi.jhsph.edu/mwccs/acknowledgements/>. A full list of participating MESA investigators and institutes can be found at <http://www.mesa-nhlbi.org>. We would also like to thank Jinshui Fan and Giovanna Fantoni for their help in the Olink proteomic analysis.

Author contributions

T.E.P. had full access to all data and takes responsibility for the accuracy of the data analysis. T.E.P., V.S.H., K.C.W., and W.S.P. contributed to the design of the study. V.S.H., R.M., M.Z., J.S.B., and L.F. contributed to the laboratory work and quality control that yielded proteomics within the discovery study (SMASH). W.S.P., K.C.W., T.T.B., J.B.M., D.A.P., G.D.K., M.P., F.J.P., and S.A.H. made substantial contributions to the acquisition and quality control of additional discovery study (SMASH) data. R.E.G., J.I.R., and S.S.R. contributed to the laboratory work and quality control that yielded proteomics within the validation study (MESA). W.S.P., S.R.H., and J.A.C.L. made substantial contributions to the acquisition and quality control of additional validation study (MESA) data. T.E.P. wrote the first draft of the manuscript. All co-authors critically reviewed the manuscript for important intellectual content, provided final approval of the version to be published, and agreed to be accountable for all aspects of the work presented.

Competing interests

T.T.B. has served as a consultant to Gilead Sciences, Merck, ViiV Healthcare, and Janssen. F.J.P. has served as a consultant and/or on the Speakers Bureau for Gilead Sciences, Merck, ViiV Healthcare, and EMD Serono. S.S.R. is a consultant to the NHLBI TOPMed Administrative Coordinating Center (Westat). J.S.B. is an advisor to Dextera Biosciences, Inc. and is a founder of and advisor to Neochromosome, Inc. and its parent company Openrons Labworks, Inc. The remaining authors declare no competing interests.

Additional information

Supplementary information The online version contains supplementary material available at <https://doi.org/10.1038/s41467-025-55911-0>.

Correspondence and requests for materials should be addressed to Tess E. Peterson.

Peer review information *Nature Communications* thanks Matthew Durstenfeld, P. Eline Slagboom, and the other anonymous reviewers for their contribution to the peer review of this work. A peer review file is available.

Reprints and permissions information is available at <http://www.nature.com/reprints>

Publisher's note Springer Nature remains neutral with regard to jurisdictional claims in published maps and institutional affiliations.

Open Access This article is licensed under a Creative Commons Attribution-NonCommercial-NoDerivatives 4.0 International License, which permits any non-commercial use, sharing, distribution and reproduction in any medium or format, as long as you give appropriate credit to the original author(s) and the source, provide a link to the Creative Commons licence, and indicate if you modified the licensed material. You do not have permission under this licence to share adapted material derived from this article or parts of it. The images or other third party material in this article are included in the article's Creative Commons licence, unless indicated otherwise in a credit line to the material. If material is not included in the article's Creative Commons licence and your intended use is not permitted by statutory regulation or exceeds the permitted use, you will need to obtain permission directly from the copyright holder. To view a copy of this licence, visit <http://creativecommons.org/licenses/by-nc-nd/4.0/>.

© The Author(s) 2025